Article

Chaotic dynamics and control in a discrete-time predator-prey system with Ivlev functional response

S. M. Sohel Rana
University of Dhaka, Dhaka-1000, Bangladesh
E-mail: srana.mthdu@gmail.com

Received 1 January 2020; *Accepted 20 February 2020*; *Published 1 June 2020*

Abstract

In this paper, a discrete-time predator-prey system with a functional response of Ivlev type is examined to reveal its chaotic dynamics. We algebraically show that the system undergoes a flip bifurcation and/or Neimark-Sacker (NS) bifurcation in the interior of $\mathbb{R}_+^2$ when one ofthe model parameter crosses its threshold value. Via application of the center manifold theorem and bifurcation theorems, we determine the existence conditions and direction of bifurcations. Numerical simulations are employed to validate analytical results which include bifurcations, phase portraits, periodic orbits, invariant closed cycle, sudden disappearance of chaotic dynamics and abrupt emergence of chaos, and attracting chaotic sets. Furthermore, maximum Lyapunov exponents and fractal dimension are computed numerically to justify the existence of chaos in the system. Finally, we apply a strategy of feedback control to control chaotic trajectories exist in the system.

Keywords predator-prey system with Ivlev functional response; bifurcations; chaos; Lyapunov exponents; feedback control.

Network Biology
ISSN2220-8879
URL: http://www.iaees.org/publications/journals/nb/online-version.asp
RSS: http://www.iaees.org/publications/journals/nb/rss.xml
E-mail: networkbiology@iaees.org
Editor-in-Chief: WenJun Zhang
Publisher: International Academy of Ecology and Environmental Sciences

1 Introduction

Predation is a very common species interaction in many ecological systems. In population ecology, the classical and dominant themes are the interaction between predator and prey species which have long been studied due to their universal existence and importance, such as resource-consumer, plant-herbivore, and phytoplankton-zooplankton forms. In recent decades, mathematical modeling is a promising approach to understand and analyze various complex dynamics of such systems in various circumstances. The dynamic complexity of predator-prey system depends on predator's rate of feeding on the prey, which is called functional response. Holling type II (others are as Holling type I, III, IV) functional response is mostly used functional response among arthropod predators. To investigate the dynamical relationship between two species predator and prey, Ivlev (1961) suggested another functional response, called Ivlev functional response:

ii. E_1 *is a source if* $\delta > max\left\{\frac{2}{r}, \frac{2}{d-1+e^{-aK}}\right\}$

iii. E_1 *is a non-hyperbolic if* $\delta = \frac{2}{r}$ *or* $\frac{2}{d-1+e^{-aK}}$.

b. if $d < 1 - e^{-aK}$ *then*

i. E_1 *is a source if* $\delta > \frac{2}{r}$,

ii. E_1 *is a saddle if* $\delta < \frac{2}{r}$,

iii. E_1 *is a non-hyperbolic if* $\delta = \frac{2}{r}$.

c. if $d = 1 - e^{-aK}$ *then* E_1 *is always non-hyperbolic.*

It is obvious that when $\delta = \frac{2}{r}$ or $\frac{2}{d-1+ e^{-aK}}$, then one of the eigenvalues of $J(E_1)$ are $\lambda_1 = 1 - r\delta$ and $\lambda_2 = 1 + \delta - d\delta - e^{-aK}\delta$ is -1 and the other is not equal to ± 1. Therefore, a flip bifurcation can occur if parameters change in small vicinity of $FB_{E_1}^1$ or $FB_{E_1}^2$:

$$FB_{E_1}^1 = \left\{(r, K, a, d, \delta) \in (0, +\infty): \delta = \frac{2}{r}, \delta \neq \frac{2}{d - 1 + e^{-aK}}, d > 1 - e^{-aK}\right\}$$

or$FB_{E_1}^2 = \left\{(r, K, a, d, \delta) \in (0, +\infty): \delta = \frac{2}{d-1+ e^{-aK}}, \delta \neq \frac{2}{r}, d > 1 - e^{-aK}\right\}$.

At $E_2(x^*, y^*)$, we write equation (6) as

$$F(\lambda) := \lambda^2 - (2 + \Delta\delta)\lambda + (1 + \Delta\delta + \Omega\delta^2) = 0,$$

where

$\Delta = 1 - d + r - \frac{2rx^*}{K} - e^{-ax^*}(1 + ay^*)$,

$$\Omega = -ae^{-ax^*}\left(-1 + e^{-ax^*}\right)y^* + \left(1 - d - e^{-ax^*}\right)\left(-\frac{rx^*}{K} + r\left(1 - \frac{x^*}{K}\right) - ae^{-ax^*}y^*\right)$$

Then $F(1) = \Omega\delta^2 > 0$ and $F(-1) = 4 + 2\Delta\delta + \Omega\delta^2$. We state following Proposition about stability criterion of E_2.

Proposition 2.3 *Suppose that fixed point* $E_2(x^*, y^*)$ *of system (3) exists. Then it is a*

(i) sink if one of the following conditions holds

(i.1) $\Delta^2 - 4\Omega \geq 0$ *and* $\delta < \frac{-\Delta - \sqrt{\Delta^2 - 4\Omega}}{\Omega}$;

(i.2) $\Delta^2 - 4\Omega < 0$ *and* $\delta < -\frac{\Delta}{\Omega}$;

(ii) source if one of the following conditions holds

(ii.1) $\Delta^2 - 4\Omega \geq 0$ *and* $\delta > \frac{-\Delta + \sqrt{\Delta^2 - 4\Omega}}{\Omega}$;

(ii.2) $\Delta^2 - 4\Omega < 0 \quad and \quad \delta > -\frac{\Delta}{\Omega}$;

(iii) non-hyperbolic if one of the following conditions holds

(iii.1) $\Delta^2 - 4\Omega \geq 0 \quad and \quad \delta = \frac{-\Delta \pm \sqrt{\Delta^2 - 4\Omega}}{\Omega}$; $\delta \neq -\frac{2}{\Delta}, -\frac{4}{\Delta}$

(iii.2) $\Delta^2 - 4\Omega < 0 \quad and \quad \delta = -\frac{\Delta}{\Omega}$;

(iv) saddle if otherwise.

From Proposition 2.3, we see that two eigenvalues of $J(E_2)$ are $\lambda_1 = -1$ and $\lambda_2 \neq \mp 1$ if condition (iii.1) holds. We rewrite the term (iii.1) as follows

$$FB^1_{E_2} = \left\{(r, K, a, d, \delta) \in (0, +\infty): \delta = \frac{-\Delta - \sqrt{\Delta^2 - 4\Omega}}{\Omega}, \quad \Delta^2 - 4\Omega \geq 0, \delta \neq -\frac{2}{\Delta}, -\frac{4}{\Delta}\right\},$$

or $FB^2_{E_2} = \left\{(r, K, a, d, \delta) \in (0, +\infty): \delta = \frac{-\Delta + \sqrt{\Delta^2 - 4\Omega}}{\Omega}, \ \Delta^2 - 4\Omega \geq 0, \delta \neq -\frac{2}{\Delta}, -\frac{4}{\Delta}\right\}$.

Therefore, a flip bifurcation can appear at E_2 if parameters vary arround the set $FB^1_{E_2}$ or $FB^2_{E_2}$.
Also we rewrite the term (iii.2) as follows

$$NSB_{E_2} = \left\{(r, K, a, d, \delta) \in (0, +\infty): \delta = -\frac{\Delta}{\Omega}, \quad \Delta^2 - 4\Omega < 0\right\},$$

and if the parameters change in small vicinity of NSB_{E_2}, two eigenvalues $\lambda_{1,2}$ of $J(E_2)$ are complex having magnitude one and then NS bifurcation can emerge from fixed point E_2.

3 Direction and Stability Analysis of Bifurcation

In this section, we will give attention to recapitulate flip and NS bifurcations of system (3) around E_2 by using the theory of bifurcation (Kuzenetsov, 1998). We set δ as a bifurcation parameter.

3.1 Flip bifurcation

Consider the system (3) at the fixed point $E_2(x^*, y^*)$ with arbitrary parameter $(r, K, a, d, \delta) \in FB^1_{E_2}$. Similar fashion for the case of $FB^2_{E_2}$. Since the parameters lie in $FB^1_{E_2}$, let $\delta = \delta_F = \frac{-\Delta - \sqrt{\Delta^2 - 4\Omega}}{\Omega}$, then the eigenvalues of positive fixed point $E_2(x^*, y^*)$ are

$$\lambda_1(\delta_F) = -1 \quad \text{and} \quad \lambda_2(\delta_F) = 3 + \Delta\delta_F.$$

The condition $|\lambda_2(\delta_F)| \neq 1$ leads to

$$\Delta\delta_F \neq -2, -4 \tag{7}$$

Using the transformation $\tilde{x} = x - x^*$, $\tilde{y} = y - y^*$ and writing $A(\delta) = J(x^*, y^*)$, we shift the fixed point (x^*, y^*) of system (3) to the origin. After Taylor expansion, system (3) reduces to

$$\begin{pmatrix} \tilde{x} \\ \tilde{y} \end{pmatrix} \to A(\delta) \begin{pmatrix} \tilde{x} \\ \tilde{y} \end{pmatrix} + \begin{pmatrix} F_1(\tilde{x}, \tilde{y}, \delta) \\ F_2(\tilde{x}, \tilde{y}, \delta) \end{pmatrix} \tag{8}$$

where $X = (\tilde{x}, \tilde{y})^T$ is the vector of the transformed systemand

$$\begin{aligned} F_1(\tilde{x},\tilde{y},\delta) &= -\tfrac{1}{6}a^2e^{-ax^*}\tilde{x}^2\delta(-3\tilde{y}+a\tilde{x}y^*) - \tfrac{r\tilde{x}^2\delta}{K} + \tfrac{1}{2}ae^{-ax^*}x\delta(-2\tilde{y}+a\tilde{x}y^*) + O(\| X \|^4) \\ F_2(\tilde{x},\tilde{y},\delta) &= \tfrac{1}{6}a^2e^{-ax^*}\tilde{x}^2\delta(-3\tilde{y}+a\tilde{x}y^*) - \tfrac{1}{2}ae^{-ax^*}x\delta(-2\tilde{y}+a\tilde{x}y^*) + O(\| X \|^4) \end{aligned} \quad (9)$$

The system (8) can be expressed as

$$X_{n+1} = AX_n + \frac{1}{2}B(X_n,X_n) + \frac{1}{6}C(X_n,X_n,X_n) + O(\| X_n \|^4)$$

where $B(x,y) = \begin{pmatrix} B_1(x,y) \\ B_2(x,y) \end{pmatrix}$ and $(x,y,u) = \begin{pmatrix} C_1(x,y,u) \\ C_2(x,y,u) \end{pmatrix}$ are symmetric multilinear vector functions of $x,y,u \in \mathbb{R}^2$ and defined as follows:

$$B_1(x,y) = \sum_{j,k=1}^{2} \left.\frac{\delta^2 F_1(\xi,\delta)}{\delta\xi_j\delta\xi_k}\right|_{\xi=0} x_jy_k = -\frac{2rx_1y_1\delta}{K} + ae^{-ax^*}\delta(-x_2y_1 - x_1y_2 + ax_1y_1y^*)$$

$$B_2(x,y) = \sum_{j,k=1}^{2} \left.\frac{\delta^2 F_2(\xi,\delta)}{\delta\xi_j\delta\xi_k}\right|_{\xi=0} x_jy_k = -ae^{-ax^*}\delta(-x_2y_1 - x_1y_2 + ax_1y_1y^*),$$

$$C_1(x,y,u) = \sum_{j,k,l=1}^{2} \left.\frac{\delta^2 F_1(\xi,\delta)}{\delta\xi_j\delta\xi_k\delta\xi_l}\right|_{\xi=0} x_jy_ku_l = -a^2e^{-ax^*}\delta(-u_2x_1y_1 - u_1(x_2y_1 + x_1(y_2 - ay_1y^*))),$$

$$C_2(x,y,u) = \sum_{j,k,l=1}^{2} \left.\frac{\delta^2 F_2(\xi,\delta)}{\delta\xi_j\delta\xi_k\delta\xi_l}\right|_{\xi=0} x_jy_ku_l = a^2e^{-ax^*}\delta(-u_2x_1y_1 - u_1(x_2y_1 + x_1(y_2 - ay_1y^*))),$$

and $\delta = \delta_F$.

Let $p,q \in \mathbb{R}^2$ be two eigenvectors of A for eigenvalue $\lambda_1(\delta_F) = -1$ such that $A(\delta_F)q = -q$ and $A^T(\delta_F)p = -p$. Then by direct calculation we get

$$q \sim \left(2 + \delta_F - d\delta_F - e^{-ax^*}\delta_F, -ae^{-ax^*}\delta_F y^*\right)^T,$$

$$p \sim \left(2 + \delta_F - d\delta_F - e^{-ax^*}\delta_F, \left(1 - e^{-ax^*}\right)\delta_F\right)^T.$$

We use the standard scalar product in $\mathbb{R}^2$ defined by $\langle p,q\rangle = p_1q_1 + p_2q_2$, to normalize p,q such that $\langle p,q\rangle = 1$. To do, we set $p = \gamma_{\mathrm{F}}\left(2 + \delta_F - d\delta_F - e^{-ax^*}\delta_F, \left(1 - e^{-ax^*}\right)\delta_F\right)^T$, where

$$\gamma_{\mathrm{F}} = \frac{1}{(2 + \delta_F - d\delta_F - e^{-ax^*}\delta_F)^2 - ae^{-ax^*}\delta_F^2y^*(1 - e^{-ax^*})}.$$

The direction of the flip bifurcation is obtained by the sign $l_1(\delta_F)$, the coefficient of critical normal form (Kuzenetsov, 1998) and is given by

$$l_1(\delta_F) = \tfrac{1}{6}\langle p, C(q,q,q)\rangle - \tfrac{1}{2}\langle p, B(q,(A-I)^{-1}B(q,q))\rangle \quad (10)$$

We state the following result on direction and stability of flip bifurcation according to above analysis.

Theorem 3.1 *If (7) holds, $l_1(\delta_F) \neq 0$ and the parameter δ changes its value around δ_F, then system (3) undergoes a flip bifurcation at positive fixed point $E_2(x^*,y^*)$. Moreover, the period-2 orbits that bifurcate from $E_2(x^*,y^*)$ are stable (resp., unstable) if $l_1(\delta_F) > 0$ (resp., $l_1(\delta_F) < 0$).*

3.2 Neimark-Sacker bifurcation

Next, we consider system (3) at fixed point $E_2(x^*, y^*)$ with arbitrary $(r, K, a, d, \delta) \in NSB_{E_2}$. From equation (6), the eigenvalues are given by

$$\lambda, \bar{\lambda} = \frac{-p(\delta) \pm \sqrt{p(\delta)^2 - 4q(\delta)}}{2}.$$

Since the parameters belong to NSB_{E_2}, so the eigenvalues will be complex and $\lambda, \bar{\lambda} = 1 + \frac{\Delta\delta}{2} \pm \frac{i\delta}{2}\sqrt{4\Omega - \Delta^2}$.

Let $\delta = \delta_{NS} = -\frac{\Delta}{\Omega}$ (11)

Therefore, we have $|\lambda| = \sqrt{q(\delta)}, \quad q(\delta_{NS}) = 1.$

From the transversality condition, we get

$$\frac{d|\lambda(\delta)|}{d\delta}\Big|_{\delta=\delta_{NS}} = -\frac{\Delta}{2} \neq 0 \quad (12)$$

Moreover, nondegenerate condition $p(\delta_{NS}) \neq 0,1$, obviously satisfies

$$\frac{\Delta^2}{\Omega} \neq 2,3 \quad (13)$$

and we have

$$\lambda^k(\delta_{NS}) \neq 1 \quad \text{for } k = 1,2,3,4 \quad (14)$$

Suppose $q, p \in \mathbb{C}^2$ are two eigenvectors of $A(\delta_{NS})$ and $A^T(\delta_{NS})$ for eigenvalues $\lambda(\delta_{NS})$ and $\bar{\lambda}(\delta_{NS})$ such that

$$A(\delta_{NS})q = \lambda(\delta_{NS})q, \quad A(\delta_{NS})\bar{q} = \bar{\lambda}(\delta_{NS})\bar{q}$$

and

$$A^T(\delta_{NS})p = \bar{\lambda}(\delta_{NS})p, \quad A^T(\delta_{NS})\bar{p} = \lambda(\delta_{NS})\bar{p}.$$

Then by direct computation we obtain

$$q \sim \left(1 + \delta_{NS} - d\delta_{NS} - e^{-ax^*}\delta_{NS} - \lambda, -ae^{-ax^*}\delta_{NS}y^*\right)^T,$$

$$p \sim \left(1 + \delta_{NS} - d\delta_{NS} - e^{-ax^*}\delta_{NS} - \bar{\lambda}, \left(1 - e^{-ax^*}\right)\delta_{NS}\right)^T.$$

For normalization of vectors p and q, we set $p = \gamma_{\mathrm{NS}}\left(1 + \delta_{NS} - d\delta_{NS} - e^{-ax^*}\delta_{NS} - \bar{\lambda}, \left(1 - e^{-ax^*}\right)\delta_{NS}\right)^T$,

where $\gamma_{\mathrm{NS}} = \frac{1}{\left(1+\delta_{NS}-d\delta_{NS}-e^{-ax^*}\delta_{NS}-\bar{\lambda}\right)^2 - ae^{-ax^*}\delta_{NS}^2 y^*\left(1-e^{-ax^*}\right)}$.

Then it is clear that $\langle p, q\rangle = 1$ where $\langle p, q\rangle = \bar{p}_1 q_2 + \bar{p}_2 q_1$ for $p, q \in \mathbb{C}^2$. Now, we decompose vector $X \in \mathbb{R}^2$as $X = zq + \bar{z}\bar{q}$, for δ close to δ_{NS} and $z \in \mathbb{C}$. Obviously, $z = \langle p, X\rangle$. Thus, we obtain the following transformed form of system (8) for $|\delta|$ near δ_{NS}:

$$z \mapsto \lambda(\delta)z + g(z, \bar{z}, \delta),$$

where $\lambda(\delta) = (1 + \varphi(\delta))e^{i\theta(\delta)}$ with $\varphi(\delta_{NS}) = 0$ and $g(z, \bar{z}, \delta)$ is a smooth complex-valued function.

After Taylor expression of g with respect to $(z,\bar{z})$, we obtain

$$g(z,\bar{z},\delta)=\sum_{k+l\geq 2}\frac{1}{k!\,l!}g_{kl}(\delta)z^k\bar{z}^l,\quad \text{with}\quad g_{kl}\in\mathbb{C},\qquad k,l=0,1,\cdots.$$

According to multilinear symmetric vector functions, the coefficients g_{kl} are

$$g_{20}(\delta_{NS})=\langle p,B(q,q)\rangle,\quad g_{11}(\delta_{NS})=\langle p,B(q,\bar{q})\rangle$$
$$g_{02}(\delta_{NS})=\langle p,B(\bar{q},\bar{q})\rangle,\quad g_{21}(\delta_{NS})=\langle p,C(q,q,\bar{q})\rangle,$$

The invariant closed curve appear in the direction which is determined by the coefficient $l_2(\delta_{NS})$ and calculated via

$$l_2(\delta_{NS})=\mathrm{Re}\left(\frac{e^{-i\theta(\delta_{NS})}g_{21}}{2}\right)-\mathrm{Re}\left(\frac{(1-2e^{i\theta(\delta_{NS})})e^{-2i\theta(\delta_{NS})}}{2(1-e^{i\theta(\delta_{NS})})}g_{20}g_{11}\right)-\frac{1}{2}|g_{11}|^2-\frac{1}{4}|g_{02}|^2,$$

where $e^{i\theta(\delta_{NS})}=\lambda(\delta_{NS})$.

Summarizing above analysis, we present the following theorem for direction and stability of Neimark-Sacker bifurcation.

Theorem 3.2 *If (13) holds, $l_2(\delta_{NS})\neq 0$ and the parameter δ changes its value in small vicinity of NSB_{E_2}, then system (3) passes through a Neimark-Sacker bifurcation at positive fixed point E_2. Moreover, if $l_2(\delta_{NS})<0$ (resp.,>0), then there exists a unique attracting (resp., repelling) invariant closed curve bifurcates from E_2.*

4 Numerical Simulations

Here, bifurcation diagrams, phase portraits, maximum Lyapunov exponents and fractal dimension of system (3) will be drawn to validate our theoretical results using numerical simulation. We assume that δ is a bifurcation parameter unless stated. We consider different set of parameter values in the following examples for bifurcation analysis.

Example 1: Flip bifurcation of system (3) with respect to bifurcation parameter δ

We fix the parameters $r=0.85, K=0.3, a=0.5, d=0.1$ and varying δ in range $3.5\leq\delta\leq 4.1$. By calculation, we find that the fixed point system (3) is $E_2(0.210721,0.533034)$, and the critical point for flip bifurcationa is $\delta=\delta_F\sim 3.70721$. At the critical bifurcation point, the two eigenvalues are $\lambda_1=-1,\lambda_2=0.835172$, $a(\delta_F)=94.4515$ and $(r,K,a,\mathrm{d},\delta)\in FB^1_{E_2}$. This verifies Theorem 3.1.

According to bifurcation diagrams shown in Fig. 1(a-b), we see that stability of fixed point E_2 happens for $\delta<\delta_F$, loses its stability at $\delta=\delta_F$ and a period doubling phenomena lead to chaos for $\delta>\delta_F$. The maximum Lyapunov exponents and fractal dimension related to Fig. 1(a-b) are computed and shown in Fig. 1(c-d). We observe that the period -2,-4, -8, -16 orbits occur for $\delta\in[3.5,4.022]$, chaotic set for $\delta\in[4.022,4.1]$. As determined by the maximum Lyapunov exponent, the status of stable, periodic or chaotic dynamics are compatible with sign in Fig. 1(c-d). The phase portraits of bifurcation diagrams in Fig. 2(a-b) for different values of δ are displayed in Fig. 2.

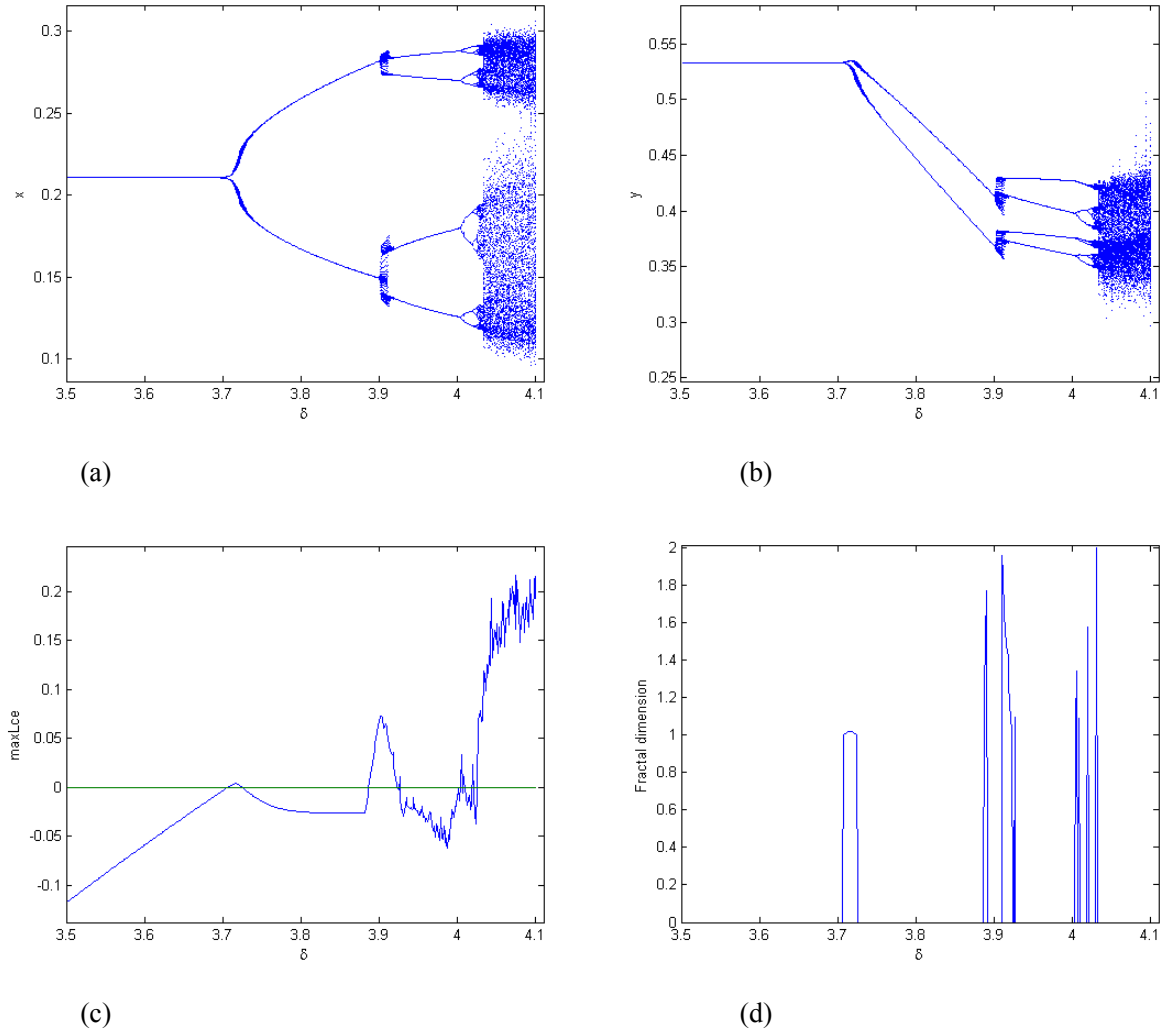

Fig. 1 Flip bifurcation and Lyapunov exponent of system (2). (a) bifurcation for prey, (b) bifurcation for predator, (c) maximum Lyapunov exponents related to (a-b), (d) Fractal dimension corresponding to (a). Initial value $(x_0, y_0) = (0.21, 0.533)$.

Example 2: Neimark-Sacker bifurcation of system (3) with respect to bifurcation parameter δ

We fix the parameters $r = 1.0, K = 1.1, a = 0.5, d = 0.2$ and varying δ in range $3.0 \leq \delta \leq 4.015$. After calculation, we observe that a NS bifurcation appears at fixed point $E_2(0.446287, 1.32611)$ for $\delta = \delta_{NS} \sim 3.22253$. Also, we have $\lambda, \bar{\lambda} = 0.44914965 \pm 0.893457i$,

$g_{20} = -0.8287361517048926 + 0.9850459369054674i$,

$g_{11} = 0.9854786934961157 - 2.334550290566222i$,

$g_{02} = 2.0014289480044947 + 3.7805618158725003i$,

$g_{21} - 1.1973007849269635 - 0.3720620335464684i$,

$$a(\delta_{NS}) = -8.120394164511106$$

and $(r, K, a, d, \delta) \in NSB_{E_2}$. This verifies Theorem 3.2.

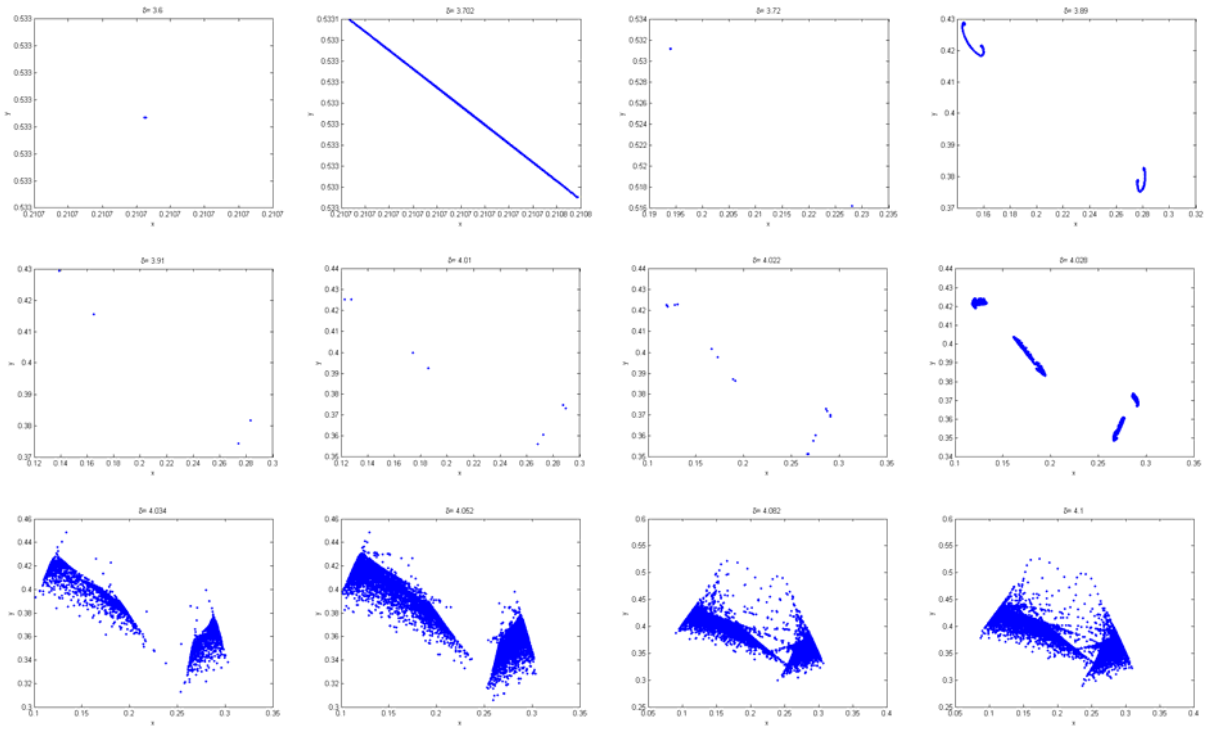

Fig. 2 Phase portraits (xy-plane) of bifurcation diagrams Fig. 1(a-b) for different values of δ.

The bifurcation diagrams shown in Fig. 3(a-b) demonstrate that stability of E_2 happens for $\delta < \delta_{NS}$, loses its stability at $\delta = \delta_{NS}$ and an attracting invariant curve appears if$\delta > \delta_{NS}$. We dispose the maximum Lyapunov exponents in Fig. 3(c) relating bifurcation in Fig. 3(a-b), which confirm the existences of chaos and period window as parameter δ varying. When δ~4.12, the sign of maximum Lyapunov exponent confirming presence of chaos. Fig. 3(d) is local amplification of Fig. 3(a) for $\delta \in [3.66,4.06]$.

The phase portraits of bifurcation diagrams in Fig. 3(a-b) for different values of δ are displayed in Fig. 4, which clearly illustrates the act of smooth invariant curve how it bifurcates from the stable fixed point and increases its radius. As δ grows, disappearance of closed curve occurs suddenly and a period -5, -10, -15, -20, and period -40 orbits appear at δ~3.85, δ~3.96, δ~4.092, δ~4.02, and δ~4.05 respectively. We also see that a fully developed chaos in system (2) occurs at δ~4.15.

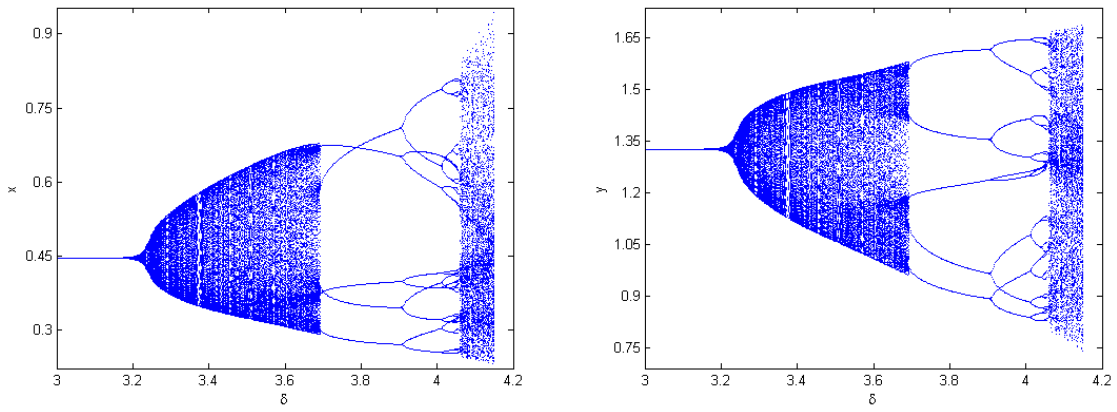

(a) (b)

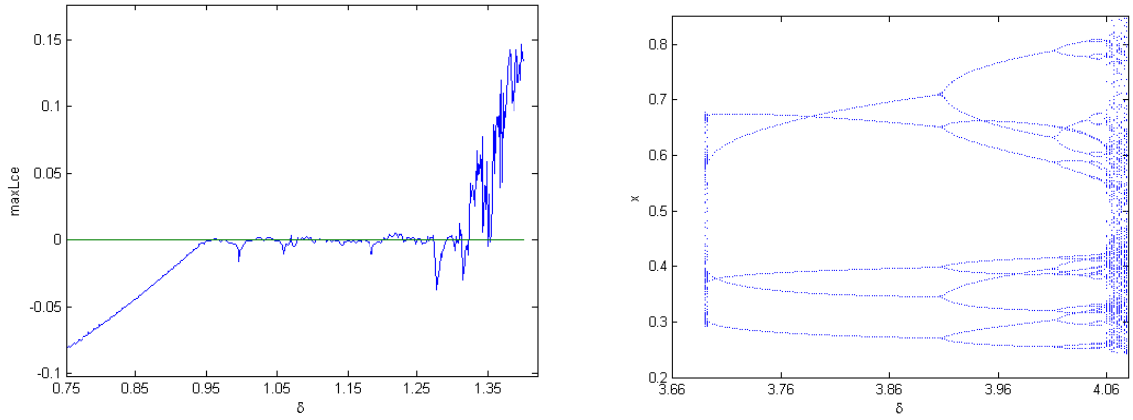

(c) (d)

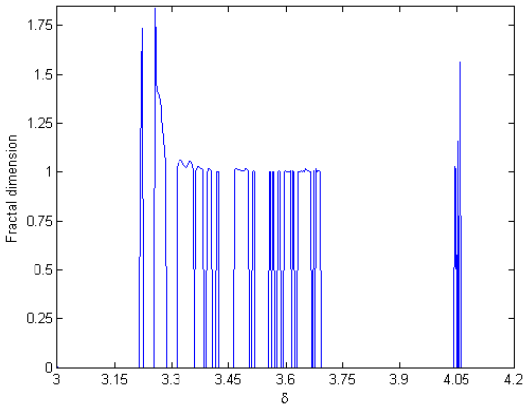

(e)

Fig. 3 NS bifurcation and Lyapunov exponent of system (2). (a) NS bifurcation for prey, (b) NS bifurcation for predator, (c) maximum Lyapunov exponents related to (a-b), (d) local amplification diagram in (a) for $\delta \in [3.0,4.15]$ (e) Fractal dimension associated with (a). Initial value $(x_0, y_0) = (0.44,1.32)$.

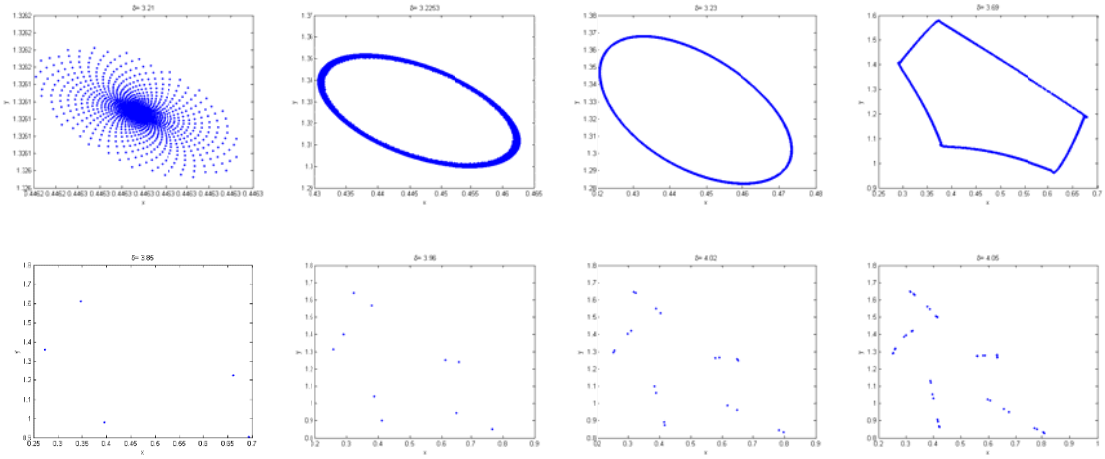

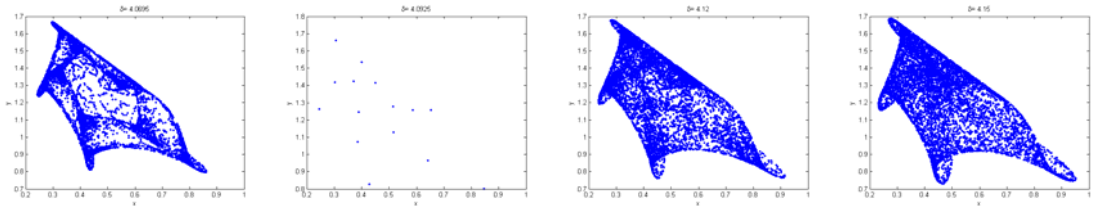

Fig. 4 Phase portraits (xy-plane) of bifurcation diagrams Fig. 3(a-b) for different values of δ.

Example 3: Neimark-Sacker bifurcation of system (3) with respect to bifurcation parameter a

With the variation of other parameter values (e.g., parameter a), the predator-prey system may exhibit richer dynamical behaviors in the Neimark-Sacker bifurcation diagram. When we set the parameter values as given in Example 2 with $\delta = 3.22253$, and varying a in range $0.4 \leq a \leq 0.67$, a new Neimark-Sacker bifurcation diagram is obtained as disposed in Fig. 5(a-b). The system undergoes a Neimark-Sacker bifurcation at $a = a_{NS}$~0.5. Similar nonlinear characteristics to Figures 3 and 4 are found in this case, such as route to chaos, invariant curves, chaotic attractors, and periodic windows. The maximum Lyapunov exponent corresponding to Fig. 5(a-b) is computed and plotted in Fig. 5(c), which confirm the existences of chaos and period window as parameter a varying. We observe from Fig. 5(a-b) that stability of system (3) happens for $a < a_{NS}$, loses its stability at $a = a_{NS}$ and an attracting invariant curve appears if $a > a_{NS}$. Also, on the route to chaos, periodic windows with period -6, -10, -12, -18, and period -24 orbits and attracting chaotic sets are found. On each branch, the predator-prey system (3) undergoes a sub-Neimark-Sacker bifurcation, flip bifurcation and periodic window with the increase of a value.

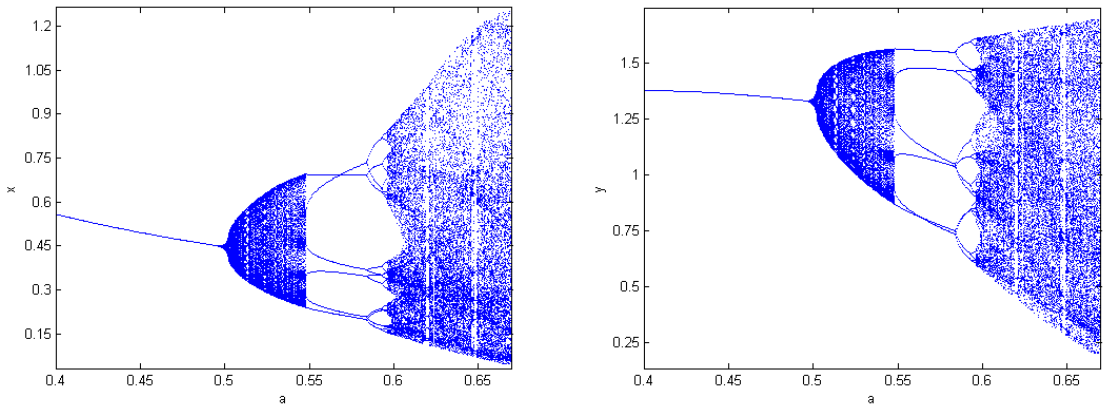

(a) (b)

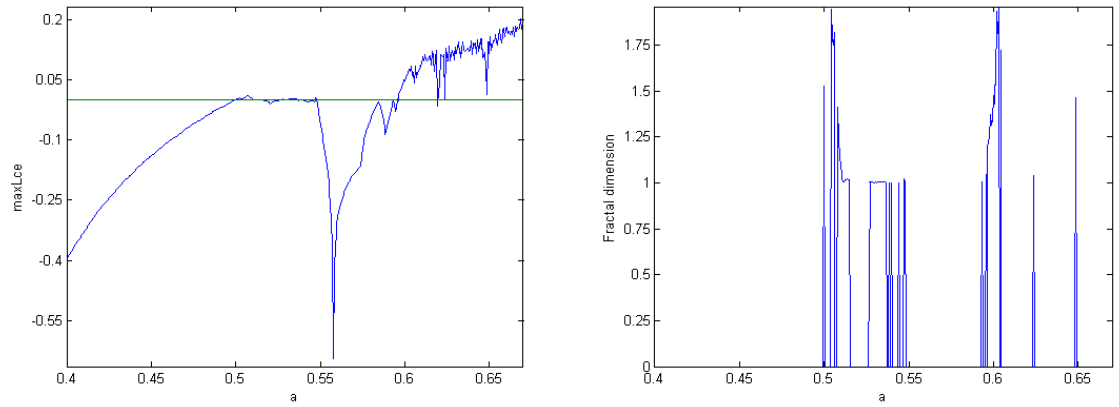

(c) (d)

Fig. 5 NS bifurcation and Lyapunov exponent of system (2). (a) NS bifurcation for prey, (b) NS bifurcation for predator, (c) maximum Lyapunov exponents related to (a-b), (d) Fractal dimension associated with (a). Initial value $(x_0, y_0) = (0.44,1.32)$.

Example 4: Maximum Lyapunov exponents for two control parameters δ and a

The dynamic complexity of system (3) can be observed when more parameters vary. We fix the parameters $r = 1.0, K = 1.1, d = 0.2$ and varying δ in range $3.0 \leq \delta \leq 4.1$, and a in range $0.44 \leq a \leq 0.64$. The sign of maximum Lyapunov exponents quantifies the existence of chaos in system (3). The 2D projection of 3D maximum Lyapunov exponents for two control parameters onto (δ, a) plane is plotted in Fig. 6. It is easy to find values of control parameters for which the dynamics of system (3) is in status of non-chaotic, periodic or chaotic. For instance, there is a chaotic dynamics for $\delta = 4.1, a = 0.5$, and the non-chaotic dynamics for $\delta = 3.85, a = 0.5$ (see Fig. 4), which are compatible with the signs of maximum Lyapunov exponents in Fig. 6. As shown in Fig. 6, we observe that the increases values of control parameters δ and a, the dynamics of system (3) changes from chaotic to non-chaotic status. Moreover, we find that the predator-prey system experiences flip bifurcation and Neimark- Sacker bifurcation simultaneously.

The measure of fractal dimensions characterizes the strange attractors of a system. By using Lyapunov exponents, the fractal dimension (Cartwright, 1999; Kaplan and Yorke, 1979) is defined by

$$d_L = j + \frac{\sum_{i=1}^{j} h_i}{|h_j|}$$

where $h_1, h_2, \ldots, h_n$ are Lyapunov exponents and j is the largest integer such that $\sum_{i=1}^{j} h_i \geq 0$ and $\sum_{i=1}^{j+1} h_i < 0$.

For our two-dimensional system (3), the fractal dimension takes the form

$$d_L = 1 + \frac{h_1}{|h_2|}, \quad h_1 > 0 > h_2 \text{ and } h_1 + h_2 < 0.$$

With parameter values as in Example 2, the fractal dimension of system (3) is plotted in Fig. 3(e). The strange attractors given in Fig. 4 and its corresponding fractal dimension illustrate that the increase values of parameter δ causes a chaotic dynamics for the predator-prey system (3).

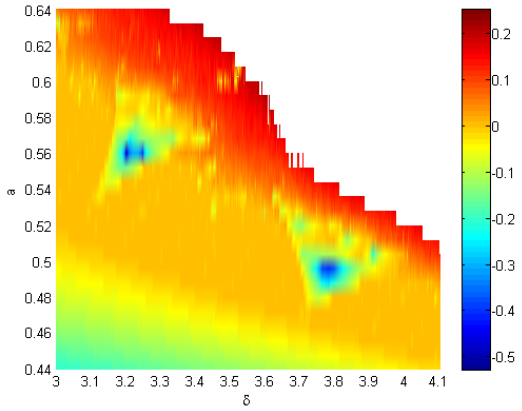

Fig. 6 Diagnostic of system (2) for control parameters δ and a. The 2D projection of 3D maximum Lyapunov exponents onto (δ, a) plane.

5 Chaos Control

To stabilize chaos at the state of unstable trajectories of system (3), a state feedback control method (Elaydi, 1996) is applied. By adding a feedback control law as the control force u_n to system (3), the controlled form of system (3) becomes

$$\begin{aligned} x_{n+1} &= x_n + \delta\left[rx_n\left(1-\frac{x_n}{K}\right) - (1 - e^{-ax_n})y_n\right] + u_n \\ y_{n+1} &= y_n + \delta[(1 - e^{-ax_n})y_n - dy_n] \end{aligned} \tag{15}$$

and

$$u_n = -k_1(x_n - x^*) - k_2(y_n - y^*)$$

where the feedback gains are denoted by $k_1$and k_2 and (x^*, y^*) represent positive fixed point of system (3).

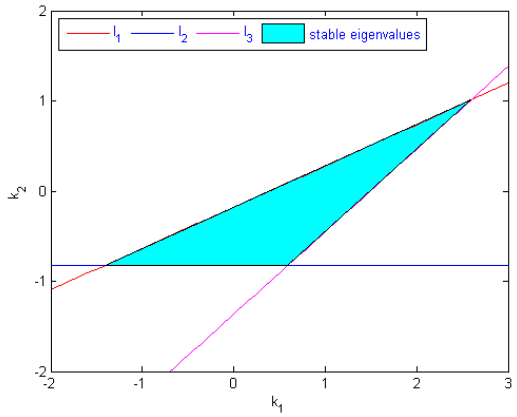

(a)

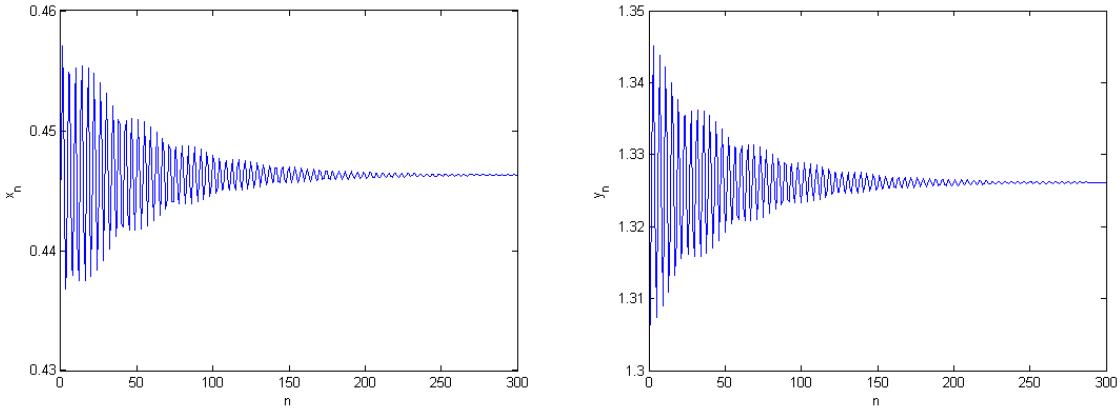

(b) (c)

Fig. 7 Control of chaotic trajectories of system (17). (a) Stability region in (k_1, k_2) plane (b-c) Time series for states x and y respectively.

The Jacobian matrix J_c of the controlled system (15) is given by

$$J_c(x^*, y^*) = \begin{pmatrix} j_{11} - k_1 & j_{12} - k_2 \\ j_{21} & j_{22} \end{pmatrix} \tag{16}$$

where $j_{pq}, p, q = 1,2$ given in (5) are evaluated at (x^*, y^*). The characteristic equation of (16) is

$$\lambda^2 - (trJ_c)\lambda + detJ_c = 0 \tag{17}$$

where $trJ_c = j_{11} + j_{22} - k_1$ and $detJ_c = j_{22}(j_{11} - k_1) - j_{21}(j_{12} - k_2)$. Let λ_1 and λ_2 be the roots of (17). Then

$$\lambda_1 + \lambda_2 = j_{11} + j_{22} - k_1 \tag{18}$$

and

$$\lambda_1\lambda_2 = j_{22}(j_{11} - k_1) - j_{21}(j_{12} - k_2) \tag{19}$$

The solution of the equations $\lambda_1 = \pm 1$ and $\lambda_1\lambda_2 = 1$ determines the lines of marginal stability. These conditions confirm that $|\lambda_{1,2}| < 1$. Suppose that $\lambda_1\lambda_2 = 1$, then from (19) we have

$$l_1: j_{22}k_1 - j_{21}k_2 = j_{11}j_{22} - j_{12}j_{21} - 1.$$

Assume that $\lambda_1 = 1$, then from (18) and (19) we get

$$l_2: (1 - j_{22})k_1 + j_{21}k_2 = j_{11} + j_{22} - 1 - j_{11}j_{22} + j_{12}a_{21}.$$

Next, assume that $\lambda_1 = -1$, then from (18) and (19) we obtain

$$l_3: (1 + j_{22})k_1 - j_{21}k_2 = j_{11} + j_{22} + 1 + j_{11}j_{22} - j_{12}j_{21}.$$

Then the lines $l_1, l_2,$ and l_3 (see Fig. 7(a)) in the (k_1, k_2) plane determine a triangular region which keeps eigenvalues with magnitude less than 1.

In order to check how the implementation of feedback control method works and controls chaos at unstable state, we have performed numerical simulations. Parameter values are fixed as $\delta = 4.12$ and rest as in

Example 2. The initial value is $(x_0, y_0) = (0.44,1.32)$, and the feedback gains are $k_1 = 0.5$ and $k_2 = 0.032$. Figures 7(b) and 7(c) show that at the fixed point $(0.210721,0.533034)$, the chaotic trajectory is stabilized.

6 Discussion

This work is concerned with the dynamics of a discrete-time predator-prey system with Ivlev functional response in the closed first quadrant $\mathbb{R}^2_+$. We prove via center manifold theorem and bifurcation theory, the system (3) can undergo a bifurcation (flip or NS) at unique positive fixed point if δ varies around the sets $FB^1_{E_2}$ or $FB^2_{E_2}$ and NSB_{E_2}. Based on Figures, we notice that the small integral step size δ can stabilize the dynamical system (3), but the large integral step size may destabilize the system producing more complex dynamical behaviors. Numerical simulations present unpredictable behaviors of the system through a flip bifurcation which include orbits of period-2, -4, -8, -16 orbits and through a NS bifurcation which include an invariant cycle, orbits of period-5, -6, -10, -12, -15, -18, -20, -24, and period-40 orbits and chaotic sets respectively. These indicate that at the state of chaos, the system is unstable and particularly, the predator goes to extinct or goes to a stable fixed point when the dynamic of prey is chaotic. We confirm about the existence of chaos through the computation of maximum Lyapunov exponents and fractal dimension. In addition, we see that the appropriate choice of parameter $a$can stabilize the dynamical system (3). The two bifurcations cause the system to jump from steady state to chaotic dynamical behavior via periodic and quasi-periodic states and trigger routes to chaos; that is, chaotic dynamics appear or disappear along with the emergence of bifurcations. Moreover, system (3) exhibits very rich nonlinear dynamical behaviors by the variation of two control parameters and one can directly observe from the two-dimensional parameter-spaces when the system dynamics will be periodic, quasi-periodic and chaotic. We observe that the increases values of control parameters δ and a, can destabilize the dynamical system (3) producing more complex dynamical behaviors, but the small values may stabilize the system. Finally, the chaotic trajectories at unstable state are controlled by implementing the strategy of feedback control. However, it is still a challenging problem to explore multiple parameter bifurcation in the system. We expect to obtain some more analytical results on this issue in the future.

References

Cartwright JHE. 1999. Nonlinear stiffness Lyapunov exponents and attractor dimension. Physics Letters A., 264: 298-304

Elaydi SN. 1996. An Introduction to Difference Equations. Springer-Verlag, New York, USA

Guo G, Li B, Lin X. 2013. Qualitative analysis on a predator-prey model with Ivlev functional response. Advances in Difference Equations, 164

He ZM, Lai X. 2011. Bifurcation and chaotic behavior of a discrete-time predator-prey system. Nonlinear Analysis and Real World Applications, 12: 403-417

He ZM, Li B. 2014. Complex dynamic behavior of a discrete-time predator-prey system of Holling-III type. Advances in Difference Equations, 180: 1-13

Ivlev VS. 1961. Experimental Ecology of the Feeding of Fishes. Yale University Press, Kentucky, USA

Kaplan JL, Yorke YA. 1979. A regime observed in a fluid flow model of Lorenz. Communications in Mathematical Physics, 67: 93-108

Kimun R. 2015. On the dynamics of predator-prey models with Ivlev's functional response. Journal of the Chungcheong Mathematical Society, 28(3): 455-472

Kooij RE. 1996. A predator-prey model with Ivlev's functional response. Journal of Mathematical Analysis

and Applications, 198(2): 473-489

Kuzenetsov YA. 1998. Elements of Applied Bifurcation Theory (2nd Ed) Springer-Verlag, New York, USA

Liu, W, Cai, D. 2019. Bifurcation, chaos analysis and control in a discrete-time predator-prey system. Advances in Difference Equations, 11

May RM. 1972. Limit cycles in predator-prey communities. Science, 177(4052): 900-902

Rana SMS. 2015. Bifurcation and complex dynamics of a discrete-time predator-prey system with simplified Monod-Haldane functional response. Advances in Difference Equations, 345

Rana SMS. 2017. Chaotic dynamics and control of discrete ratio-dependent predator-prey system. Discrete Dynamics in Nature and Society, 4537450

Rana SMS. 2019. Bifurcations and chaos control in a discrete-time predator-prey system of Leslie type. Journal of Applied Analysis and Computation, 9(1): 31-44

Rana SMS. 2019. Dynamics and chaos control in a discrete-time Holling-Tanner model. Journal of the Egyptian Mathematical Society, 27: 48

Rana SMS, Kulsum U. 2017. Bifurcation analysis and chaos control in a discrete-time predator-prey system of Leslie type with simplified Holling type IV functional response. Discrete Dynamics in Nature and Society, 2: 1-11

Sugie J. 1998. Two-parameter bifurcation in a predator-prey system of Ivlev type. Journal of Mathematical Analysis and Applications, 217(2): 349-371

Zhao M, Li C, Wang J. 2017. Complex dynamic behaviors of a discrete-time predator-prey system. Journal of Applied Analysis and Computation, 7: 478-500

Zhao M, Xuan Z, Li C. 2016. Dynamics of a discrete-time predator-prey system. Advances in Difference Equations, 2016: 191